The distortion of two $FePO_4$ polymorphs with high pressure

SUPPLEMENTARY INFORMATION

Craig L Bull,[a,*] Chiristopher J Ridley,[a] Nicholas P Funnell,[a] Craig W Wilson, [b] Simon G MacLeod, [b]

[a] ISIS Facility, Rutherford Appleton Laboratory, Harwell Science and Innovation Campus, Didcot, OX11 0QX, UK

[b] AWE, Aldermarston, Reading, RG7 4PR, UK

[*]To whom correspondence should be addressed;

E-mail: craig.bull@stfc.ac.uk

Submitted to Materials Advances

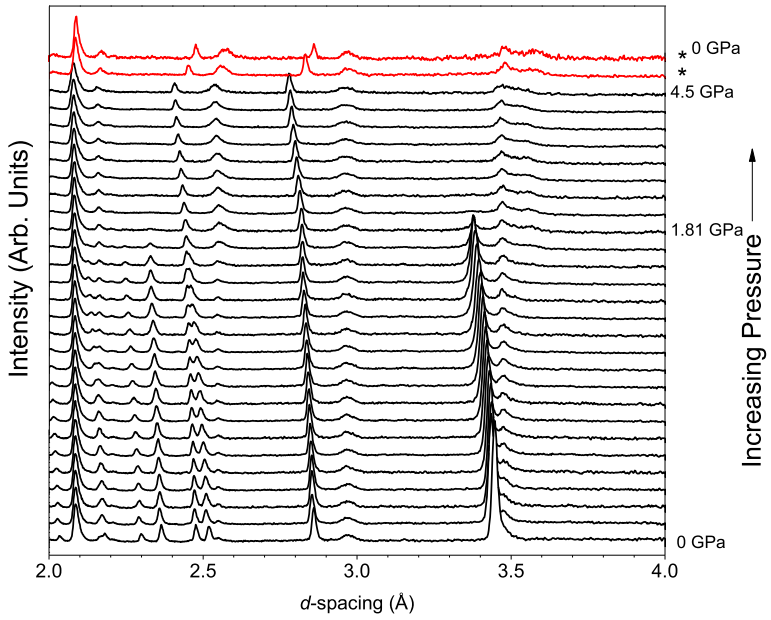

Figure S1: Neutron diffraction patterns of $FePO_4$-I with increasing pressure. The top red diffraction patterns are $FePO_4$-I recovered back to ambient pressure measured within the Paris-Edinburgh cell. Figure S6 shows the recovered sample measured on Polaris instrument upon removal from the TiZr gasket.

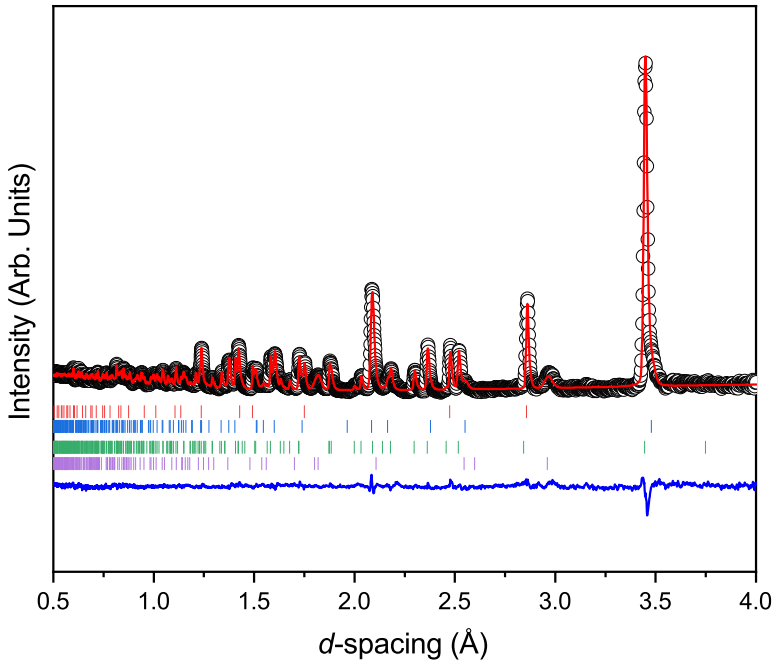

Figure S2: Example Rietveld refinement of $FePO_4$-I in situ. Data shown as open circles, Rietveld fit as solid red line, the blue trace the residual from the refinement. The vertical tick marks show the positions of the diffraction peaks from the phases within the refinement and represent from top to bottom: lead pressure marker, Al_2O_3 from anvil, ZrO_2 from anvil and trigonal $FePO_4$.

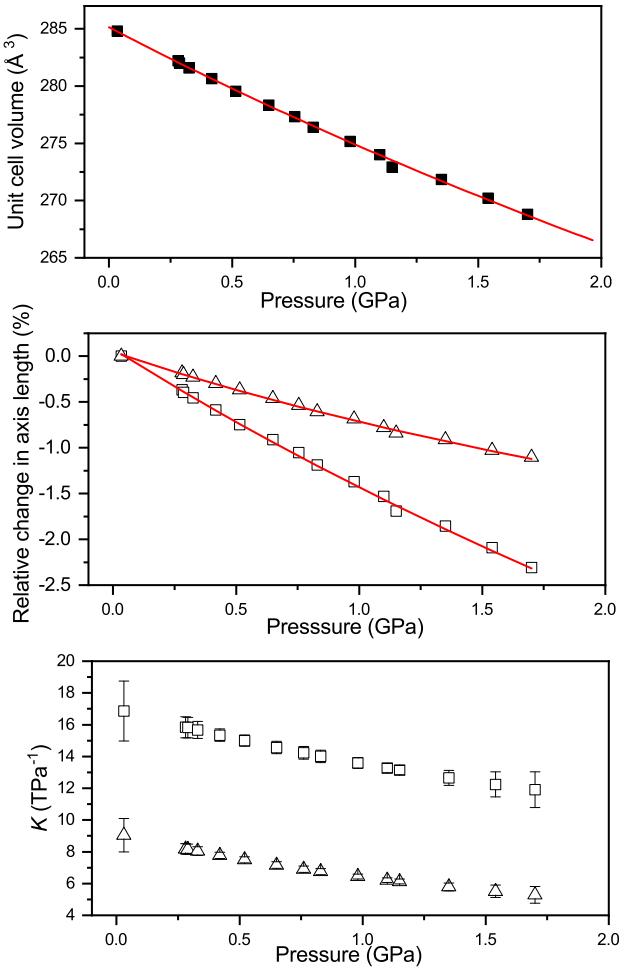

Figure S3: Top: Variation in unit-cell volume of $FePO_4$-I with increasing pressure as shown by the solid squares. The solid line is the determined equation of state fitted to the experimental data. Middle: Relative changes in unit-cell lengths of, and Bottom: unit-cell axial-compressibility of $FePO_4$-I with increasing pressure. The a-axis is shown by the open squares and c by open triangles.

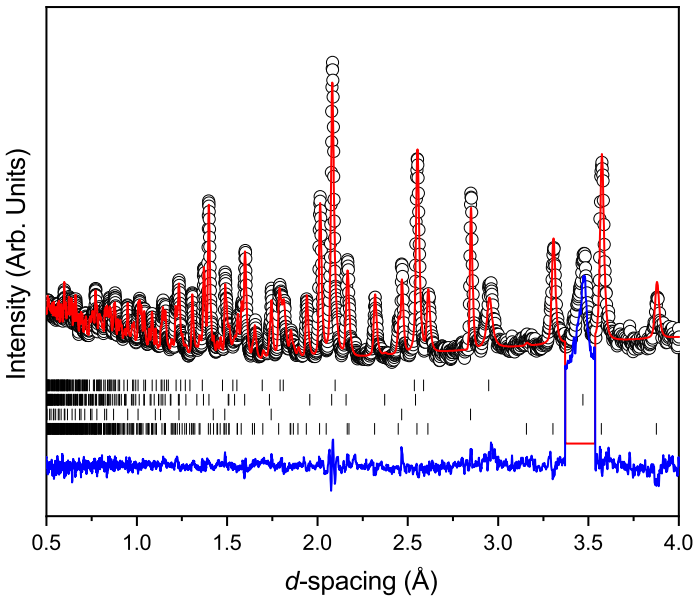

Figure S4: Example Rietveld refinement of $FePO_4$-II in situ. Data shown as open circles, Rietveld fit as solid red line, the blue trace the residual from the refinement. The vertical tick marks show the positions of the diffraction peaks from the phases within the refinement and represent from top to bottom: lead pressure marker, Al_2O_3 from anvil, ZrO_2 from anvil and orthorhombic $FePO_4$. At $\sim$3.4 Å there is a highly strained anvil reflection which is excluded from the refinement.

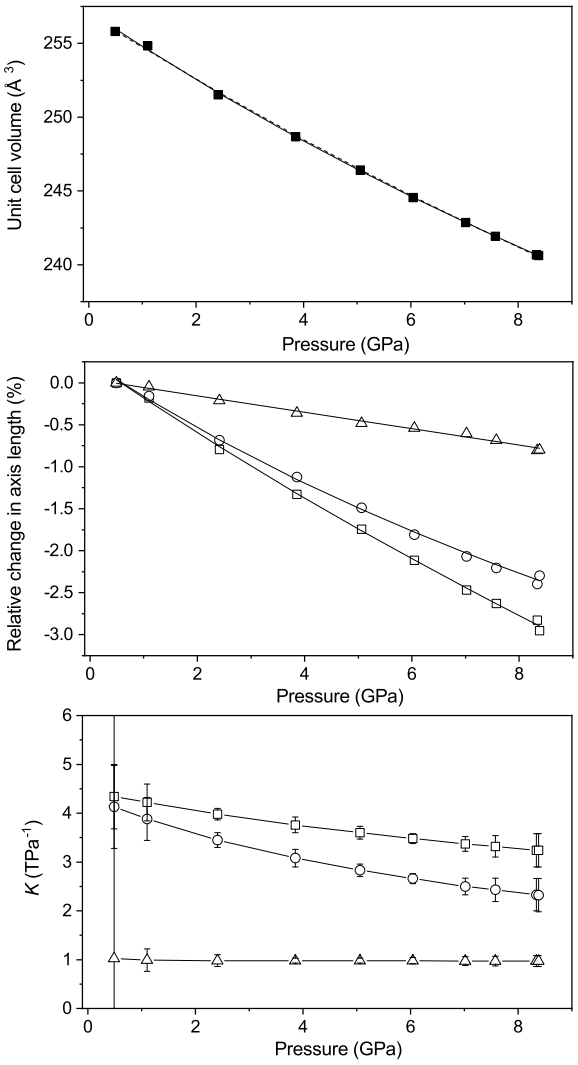

Figure S5: Top: Variation in unit-cell volume of $FePO_4$-II with increasing pressure as shown by the solid squares. The solid line is the determined equation of state fitted to the experimental data. Middle: Relative changes in unit cell axis lengths of $FePO_4$-II with increasing pressure. The a-axis is shown by the open squares, b by open circles and c by open triangles. Bottom: Compressibility of each unit-cell axis of $FePO_4$-II with increasing pressure. The a-axis is shown by open squares , b by open circles and c by open triangles.

Table S1: Determined structural parameters from the refinement of $FePO_4$-I at high pressure. The symmetry for all pressure points detailed is trigonal (space group $P3_121$) with $\alpha = \beta = 90°$ and $\gamma = 120°$. The Fe is sat on the $3a$ Wyckoff site $y = 0$ and $z = \frac{1}{3}$. The P on the $3b$ site with $y = 0$ and $z = \frac{1}{6}$. Both O1 and O2 are sat on the $6c$ Wyckoff position.

Pressure (GPa)	0.033	0.286	0.28	0.325	0.417	0.515	0.649	0.755
$a = b$ (Å)	5.03333(15)	5.01352(15)	5.01483(18)	5.01046(15)	5.00385(17)	4.9957(2)	4.98746(18)	4.98034(16)
c (Å)	11.2420(6)	11.2197(6)	11.2218(7)	11.2163(6)	11.2086(6)	11.2008(9)	11.1902(7)	11.1816(6)
Volume (Å^3)	246.652(10)	244.228(10)	244.403(12)	243.857(10)	243.046(12)	242.091(17)	241.062(12)	240.189(11)
Fe x	0.4566(9)	0.4553(9)	0.4543(10)	04547(9)	04547(9)	0.4531(14)	0.4531(10)	0.4519(9)
P x	0.460(2)	0.4660(19)	0.467(2)	0.4665(19)	0.464(2)	0.461(3)	0.463(2)	0.462(2)
O1 x	0.4194(16)	0.421315)	0.4237(19)	0.4200(15)	0.4193(16)	0.425(2)	0.4177(16)	0.4178(15)
y	0.3191(12)	0.3219(11)	0.3223(13)	0.4202(11)	0.3224(12)	0.3215(16)	0.3232(12)	0.3253(11)
z	0.3962(4)	0.3960(3)	0.3953(4)	0.3953(3)	0.3951(4)	0.3948(5)	0.3944(4)	0.3935(3)
O2 x	0.4105(16)	0.4082(15)	0.4056(19)	0.4077(16)	0.4104(17)	0.404(2)	0.4098(17)	0.4096(16)
y	0.2640(11)	0.2657(10)	0.2647(11)	0.2661(10)	0.2672(12)	0.2639(15)	0.2691(11)	0.2698(11)
z	0.8750(5)	0.8739(5)	0.8746(6)	0.8739(5)	0.8733(5)	0.8726(7)	0.8732(5)	0.8728(5)

Pressure (GPa)	0.829	0.979	1.1	1.15	1.35	1.54	1.7
$a = b$ (Å)	4.97357(19)	4.96443(18)	4.95623(18)	4.94813(18)	4.9400(2)	4.9281(2)	4.9171(2)
c (Å)	1.1738(7)	11.1650(7)	11.1545(7)	11.1477(7)	11.1398(8)	11.1265(8)	11.1179(9)
Volume (Å^3)	239.369(13)	238.302(12)	237.293(13)	236.372(13)	235.426(15)	243.013(15)	232.798(17)
Fe x	0.4524(11)	0.4521(10)	0.4517(10)	0.5438(10)	0.4534(11)	0.4529(10)	0.4545(11)
P x	0.460(2)	0.457(2)	0.451(2)	0.441(2)	0.442(2)	0.435(2)	0.433(3)
O1 x	0.4182(17)	0.4177(17)	0.4165(16)	0.4144(15)	0.4145(19)	0.4161(19)	0.419(2)
y	0.3239(12)	0.3240(12)	0.3253(12)	0.3241(12)	0.3232(14)	0.3250(14)	0.3276(15)
z	0.3943(4)	0.3937(3)	0.3939(3)	0.3937(3)	0.3932(4)	0.3929(4)	0.3932(4)
O2 x	0.4085(18)	0.4082(16)	0.4090(17)	0.4084(16)	0.4073(19)	0.4030(19)	0.398(2)
y	0.2718(12)	0.2720(11)	0.2759(12)	0;2769(12)	0.2780(13)	0.2820(12)	0.2825(14)
z	0.8716(6)	0.8720(5)	0.8716(5)	0.8713(5)	0.8704(6)	0.8714(5)	0.8705(6)

Table S2: Determined structural parameters from the refinement of $FePO_4$-II at high pressure. The symmetry for all pressure points detailed is orthorhombic (space group $Cmcm$) . The Fe is sat on the $4a$ Wyckoff site with $x = y = z = 0$. The P on the $4c$ site with $x = 0$ and $z = \frac{1}{4}$. O1sited on the $8f$ Wyckoff site with $x = 0$ and O2 sat on the $8g$ Wyckoff position with $z = \frac{1}{4}$.

Pressure (GPa)	0.5	1.1	2.4	3.9	5.1	6.0	7.0	7.6	8.3	8.4
a (Å)	5.2230(3)	5.2205(4)	5.2120(4)	5.2041(5)	5.1978(6)	5.1947(7)	5.1897(12)	5.1853(13)	5.1775(15)	5.1756(19)
b (Å)	7.7548(4)	7.7427(5)	7.7019(6)	7.6677(7)	7.6393(8)	7.6147(10)	7.5933(16)	7.5836(17)	7.569(2)	7.576(3)
c (Å)	6.3158(4)	6.3035(5)	6.2656(5)	6.2319(7)	6.2057(8)	6.1824(10)	6.1608(15)	6.149(17)	6.1373(19)	6.129(2)
Volume (Å^3)	255.810(16)	254.829(18)	251.52(2)	248.67(3)	246.41(3)	244.55(4)	242.78(6)	241.82(7)	240.50(8)	240.33(10)
P y	0.3551(6)	0.3558(7)	0.3571(8)	0.3582(9)	0.3591(11)	0.3583(14)	0.358(2)	0.3595(15)	0.3593(17)	0.36(2)
O1 y	0.2436(4)	0.2438(4)	0.24400(4)	0.2462(5)	0.2479(5)	0.2493(7)	0.2495(10)	0.2482(11)	0.2477(13)	0.2501(17)
z	0.0487(4)	0.0493(5)	0.0499(5)	0.0483(6)	0.0483(6)	0.0473(7)	0.0455(11)	0.0482(12)	0.498(14)	0.0483(19)
O2 x	0.2472(5)	0.2469(6)	0.2497(7)	0.2495(7)	0.2495(8)	0.2478(10)	0.2470(13)	0.2507(13)	0.2451(14)	0.2448(18)
y	0.4678(4)	0.4681(4)	0.4714(4)	0.4714(5)	0.4770(6)	0.4814(8)	0.4833(13)	0.4927(15)	0.5076(15)	0.5081(19)

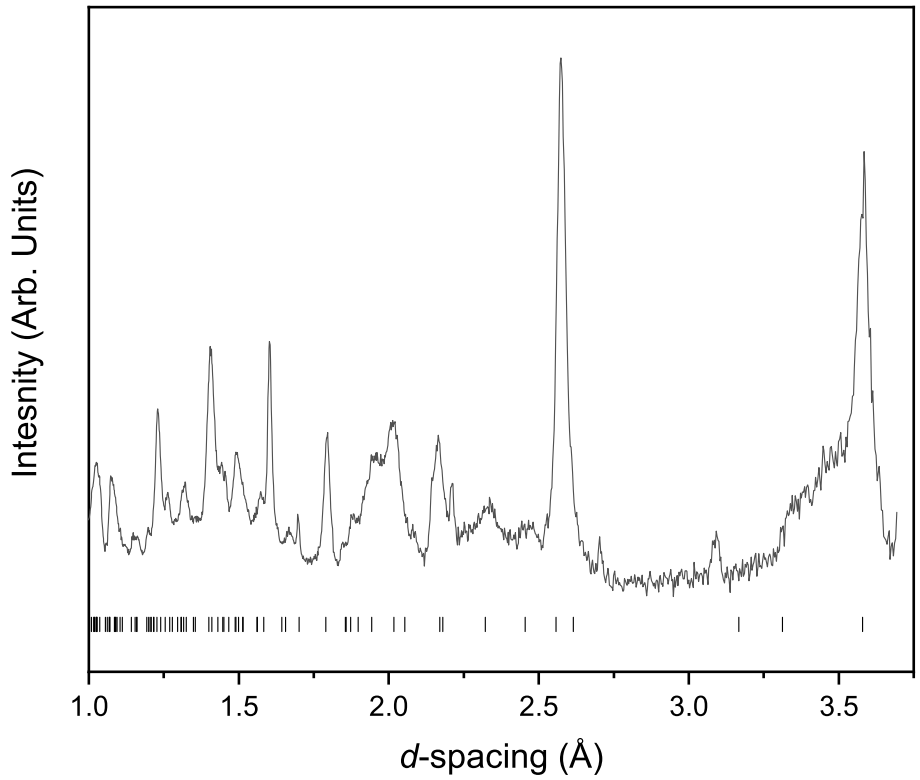

Figure S6: Neutron powder diffraction pattern of $FePO_4$Ir (recovered $FePO_4$-I following compression of $\sim$4 GPa hydrostatically and recovery to ambient pressure.

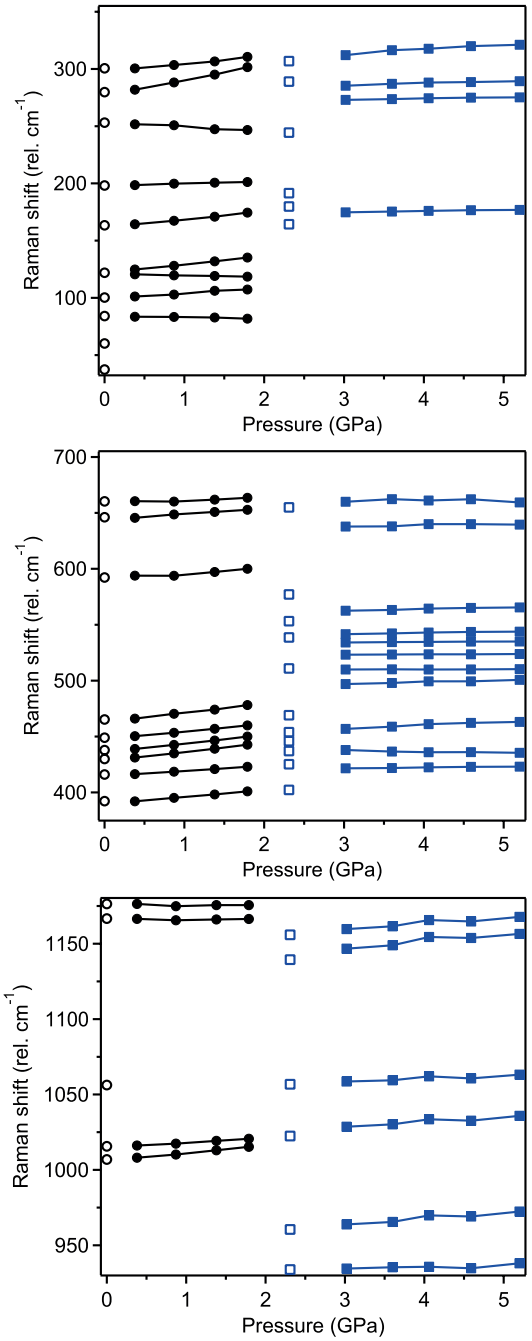

Figure S7: Variation in determined peak position of Raman spectra of $FePO_4$-I with increasing pressure

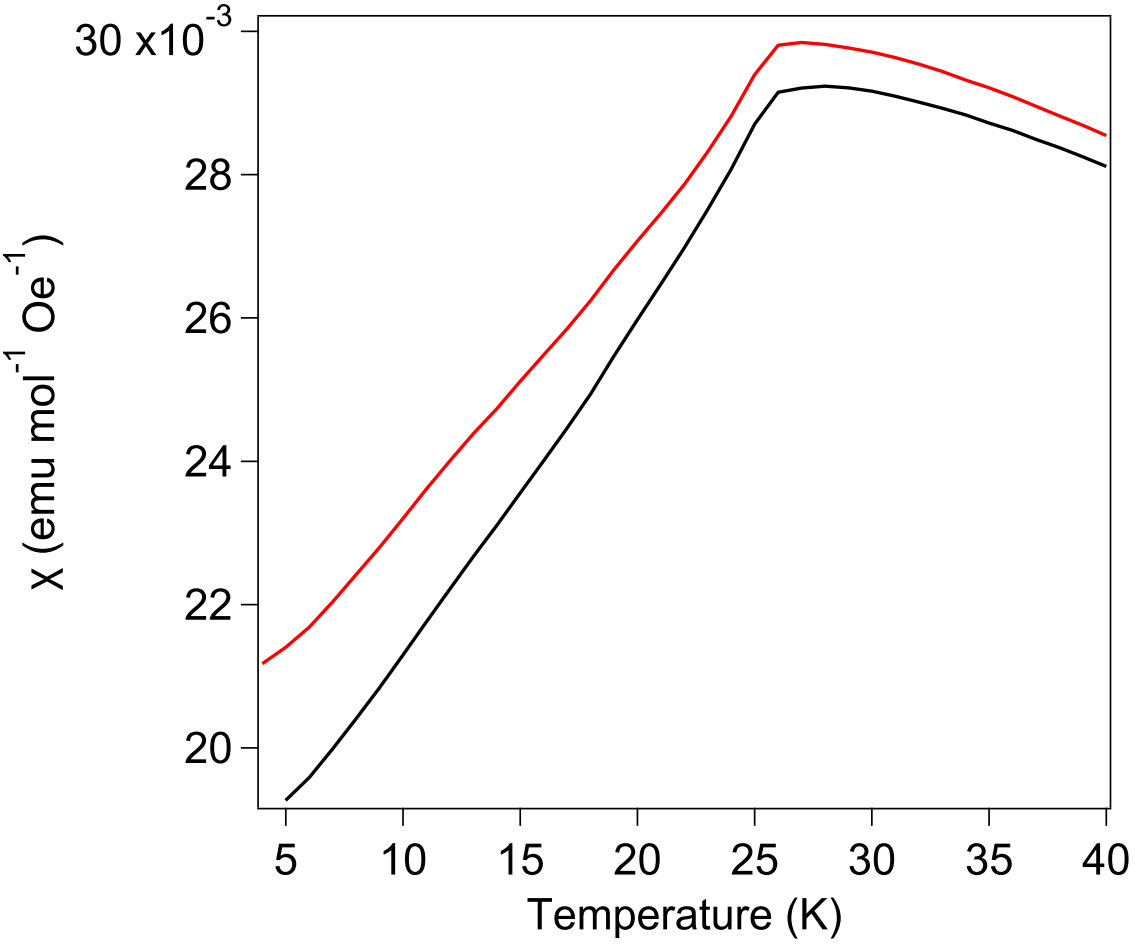

Figure S8: Low temperature region of FC and ZFC magnetic susceptibility of $FePO_4$